INTERPRETATION OF THE 9,10-ANTRAQUINONE CHROMOPHORE BY CONFIGURATION ANALYSIS*

Jürgen FABIAN and Miloš NEPRAŠ

Chemistry Department, Technical University, Dresden, GDR and Research Institute for Organic Syntheses, 532 18 Pardubice - Rybitví, ČSSR

Received May 30th, 1979

In order to disclose the validity of former phenomenological interpretations and rules concerning the spectral absorption feature of antraquinone dyes, electronic wave functions of 9,10-antraquinone and some derivatives have been subjected to the configuration analysis (CA). The calculations demonstrate the possibilities and limitations of the different approaches. The results enable us to make the consistent interpretation in terms of molecular fragments.

Because of their considerable importance as synthetic and naturally occurring dyes, the spectral feature of 9,10-antraquinones has attracted much interest[1-3]. The parent compound was extensively studied experimentally as well as theoretically[4-9]. The more recent theoretical results are in complete agreement with polarization measurements[6,10-12]. Whereas the weak longest-wavelength absorption of 9,10-antraquinone arises from a n-π^* transition[9], π—π^* transitions determine the intense shorter-wavelength absorptions[4-8]. Donor substituents bring about considerable spectral shifts[13-15]. Extremly strong red shift is observed with multiple amino substitution[16-20]. Spectral data of aminoanthraquinones were reproduced by calculations within the PPP approximation[19-22]. These results are also satisfactory in line with polarization spectra[19,20].

However, in spite of the great success in reproducing the main absorption feature of antraquinones and in interpreting individual absorption bands, less progress has been made in rationalizing empirical rules describing spectrum structure relationships. For that reason, spectral effects of anthraquinones are commonly discussed in terms of phenomenological conceptions rather than in terms of quantum chemical approximations.

The small contribution of quantum chemistry to a conceptual understanding results mainly from the fact that theoretical studies mostly consider to π-system as a whole, whereas phenomenological conceptions refer to the presence of certain molecular fragments or their combinations. Thus Morton and Earlam[23] attributed absorption bands of 1,4-naphthoquinone and 9,10-anthraquinone either to the benzoyl or to the quinone sub-structure. Based on this approach, the absorption spectra of anthraquinones were discussed in terms of "benzenoid bands" and "quinoid bands"[12,15,17,24]. Anthraquinone absorption bands at about 320 nm and 250 nm were labelled as "benzenoid band" and the absorption band at 270 nm as "quinoid band". Both the "quinoid" and "benzenoid band" are assumed to be retained in spectra of substituted anthraquinones. However, whereas the 320 nm absorption of the benzoyl fragment persists upon single substitution, it vanishes with substitution at both benzene fragments. Popov and coworkers[25]

* Part VIII in the series Electronic Structure and Properties of Polynuclear Aromatic Ketones and Quinones; Part VII: This Journal *42*, 2343 (1977).

discussed this finding by means of perturbation theory in terms of local excitations at the benzoyl fragments and amino-to-benzoyl charge transfer excitations.

The longest-wavelength absorption of hydroxy- and aminoanthraquinones is generally considered as substituent-to-anthraquinone charge transfer band, which appears in addition to the UV anthraquinone absorption bands[13,15]. This assignment is accordant with the marked solvent dependence of the longest-wavelength absorption. An alternative interpretation has been advanced by Dähne and Leupold[26]. They interpreted the appearance of the colour band as arising from polymethine subunits.

Spruit distinguished between delocalized "fundamental bands" and localized "partial bands"[27]. Spectral similarities between anthraquinones and correspondingly substituted naphthoquinones lead him to assume that the two naphthoquinoid halves of the anthraquinone molecule absorb practically independent of each other. Thus the spectrum of 9,10-anthraquinone is considered as superposition of two 1,4-naphthoquinone spectra. In accordance with this picture the intensity of the visible absorption bands of 1,5- and 1,8-disubstituted anthraquinones is approximately twice that of the corresponding 1-substituted anthraquinones[13,17,27] ("additivity rule").

According to Hartmann and Lorenz[16] the carbonyl groups interrupt the π-delocalization. The position of the longest-wavelength $\pi\pi^*$ absorption bands of unsymmetrically annelated quinones is assumed to arise from the larger benzenoid residue. Studies on acene quinones supported "Hartmann's rule"[28]. This kind of consideration directs attention to the acene fragments. Thus the excited state responsible for the first anthraquinone absorption band has been attributed to a L_b-type excited state of the benzene fragments[10,29]. Drott and Dearman[10] explained the occurrence of localized transitions in terms of weakly interacting units using Platt's spectroscopic moment theory. To compare the absorption feature of anthraquinone with that of other aromatic ketones, "molecules-in-molecule" calculations based on ketone and benzene fragments were performed[7,8]. Finally, the anthraquinone spectrum was compared with that of anthracene[30]. The appearance of a very intense absorption maximum at about 250 nm in both spectra suggested a similar electronic origin of these absorption bands.

The phenomenological assignments mentioned above were mostly based on the position and intensity of absorption bands and, in some cases, on the polarization spectra of the compounds under comparison. However, since numerical correspondence between experimental findings may be fortuitous, the phenomenological interpretations necessitate a theoretical justification.

At first glance it might be believed that the validity of the interpretations can immediately be judged from refined calculations, for example, from PPP calculations. However, due to the fact that the π-electronic systems are described in terms of delocalized orbitals, a partial localization of electronic transitions is difficult to recognize by a rough inspection of the wave functions only.

There are two ways to overcome this difficulty[31,32]: First, by evaluating the localized nature of the electronic transitions by virtue of the matrices of molecular orbitals and the configuration interaction expansion, the difference of the density matrices between ground and excited state or the squared transition density matrices. Secondly, by evaluating the localized nature of the electronic states which are involved in the excitation with respect to those of related and topologically equivalent π-systems.

For a straight comparison between the spectral properties of different compounds the last mentioned approach proved to be very useful[33]. In particular the so-called configuration analysis (CA) of Baba, Suzuki and Takemura[34] provides correlation diagrams and makes it possible to select the most favourable molecular partitioning ("analytic approach"). In the case of a proper choice of the reference structure, the energy levels of the considered molecule can be satisfactorily derived from those of molecular fragments ("synthetic approach").

The purpose of the present paper is to analyse in terms of molecular subunits the electronic structure of 9,10-anthraquinone *I* and some derivatives such as 2-nitro--9,10-anthraquinone *II*, 1-amino-9,10-anthraquinone *III*, 2-amino-9,10-anthraquinone *IV*, indanthrone *V* and isoindanthrone *VI*.

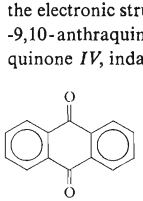

I

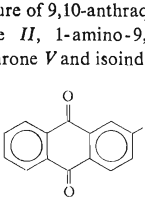

II

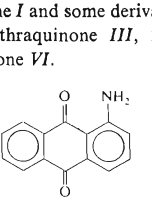

III

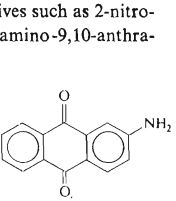

IV

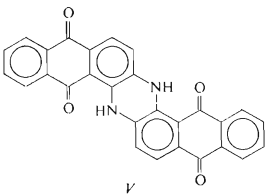

V

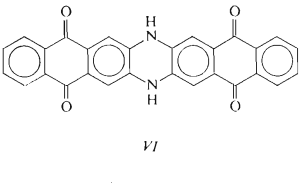

VI

In order to rationalize the electronic structure of the anthraquinone parent chromophore, five different composite molecule models are considered; *i*) anthraquinone as being composed from two benzene and two carbonyl fragments (model A), *ii*) anthraquinone as being composed from 1,4-benzoquinone and two butadiene fragments (model B), *iii*) anthraquinone as being composed from 1,4-naphthoquinone and one butadienen fragment (model C), *iv*) anthraquinone as being composed from two benzoyl moities (model D) and *v*) anthraquinone as being composed from anthracene and two oxygen atoms (model E)

The compounds *II* to *VI* are mainly regarded as derivatives of 9,10-anthraquinone, *i.e.* with respect to molecular fragments described by model F and G, respectively.

In order to examine the relevance of the coupled polymethine reference structure, indanthrone *V* was alternatively analyzed according to model H. Both *V* and *VI* are finally considered as coupled 2-aminoanthraquinones (model I).

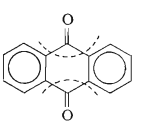

model A

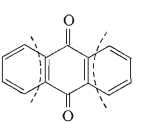

model B

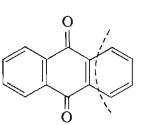

model C

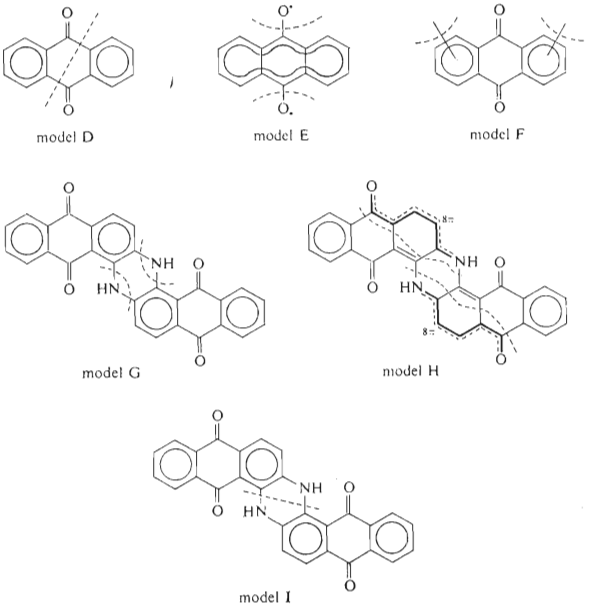

CALCULATIONS

The electronic transitions were calculated by the Pariser–Parr–Pople (PPP) method. All calculations were carried out for idealized standard geometries (all CO bond lengths equal 1·22 Å, all CC bond lengths equal 1·4 Å, regular hexagon) using the Mataga–Nishimoto approximation for the two-center repulsion integrals. The oxygen and nitrogen parameters used ($I_O - I_C =$ $= 5{\cdot}86$ eV, $Z_O^c = 1$, $\gamma_{OO} = 14{\cdot}58$ eV, $\beta_{CO} = -2{\cdot}782$ eV. $I_N - I_C = 11{\cdot}71$ eV, $Z_N^c = 2$, $\gamma_{NN} =$ $= 12{\cdot}98$ eV, $\beta_{CN} = -2{\cdot}318$ eV) are those employed in former papers by one of us (J. F.). To take into account the different strength of the CC-bonds in quinoid structures, the resonance integral β_{CC} was evaluated by a variable β-procedure[35]. The number of singly excited configurations which enter into the configuration interaction is specified below.

In order to characterize the nature of the electronic transitions two different procedures have been used. First, the amount of locally excited and charge transfer transition was derived from the MO and CI expansion (matrices **C** and **U**) of the π-system under study, as described by Ohta, Kuroda and Kunii (OKK analysis)[36]. Secondly, the degree of localization was evaluated from the diagonal elements of the squared density matrices ($\mathbf{D}^2$), as proposed by Lusanov, Sukhorukov and Umanskii (LSU analysis)[37]. Nepraš and Titz[44] have determined the character of $\pi\pi^*$ transi-

tions at a series of *p*-acenequinones from the changes of LCI π-electron densities on different subsystem in the $S_0 \rightarrow S_a$ transition.

The nature of the electronic states is defined by the CA analysis[34]. This method refers the wave functions of a given π-system (matrices **C** and **U**) to those of the reference system (matrices $\mathbf{C}^0$ and $\mathbf{U}^0$) (ref.[37]). A schematic outline of the computational steps is given in Fig. 1.

MOs are compared in the first step of the calculation. As long as topologically equivalent π-systems are compared, the MOs of the considered system and the MOs ψ^0 of the reference system are related by the unitary matrix **B** (molecular orbital analysis). Through calculations of appropriate determinants of the matrix **B**, the coefficients of the **L** matrix are obtained next. These coefficients define each configuration of the system concerned in terms of configurations constructed from MOs of the reference system. The final step of calculations takes into account the CI matrices of both π-systems under comparison. The resulting matrix **M** contains the coefficients of the considered state wave functions in terms of those of the reference system.

Due to the limited number of electronic configurations the expansion of the state functions ψ in terms of the J state functions ψ^0 is incomplete and the sum of the squared coefficients m_{IJ}^2 of each electronic state I is lower than unity. Introducing the term r_M, this relationship is expressed by

$$r_M(I) = \sum_J m_{IJ}^2 \leqq 1 \,.$$

Thus the r_M-values indicate the appositeness of the reference states. According to our former studies satisfactory interpretations are attained if the r_M-values exceed about 0·95 (95%) and 0·8 (80%) for the ground and excited state, respectively.

The fragment reference systems according to the models A to I are topologically equivalent and iso-π-electronic. In that case the reference states (or configurations) are the nobond (NB) ground state, locally ecxited (LE) states and charge-transfer (CT) states.

Alternatively, the same type of configurations can be used as basic set to generate molecular state functions. This method was introduced by Longuet-Higgins and Murrell (LHM method)[38,39]. Only if the CA calculations evidence an proper choice of molecular fragments, do the results of the LHM calculation approach those of the PPP-CA calculation. The results become nearly equivalent if the r_M-values of the configuration analysis exceed about 0·99 (99%) and 0·95 (95%) for the ground and excited state, respectively.

For the sake of interpretation, a limited number of singly excited reference states were employed in this paper. The number varied with the problem under study. Details are given below.

RESULTS AND DISCUSSION

The Anthraquinone Parent Chromophore

In order to define proper wave functions, anthraquinone (*I*) has been calculated in PPP approximation with different configuration interaction expansions. As demonstrated in Table I and Fig. 2, the results remain almost unchanged when the number of singly excited configurations is increased from 16 to 64 (all singly excited configurations). Therefore, all subsequent analyses have been performed within an approximation in which the number of configurations is limited to 16.

According to our calculation and in complete accordance with former theoretical results[4-6] the first intense absorption band at 320 nm results from the $S_0 \rightarrow S_1$

$\pi-\pi^*$ transition. The shorter wavelength absorption bands centered at 270 nm and 250 nm are brought about by the $S_0 \rightarrow S_4$ and $S_0 \rightarrow S_5$ $\pi-\pi^*$ transitions, respectively. The $S_0 \rightarrow S_2$ and $S_0 \rightarrow S_3$ $\pi-\pi^*$ transitions are electronically forbidden.

In the following, the nature of these electronic transitions is considered first and the nature of the pertinent electronic states after that.

The OKK analysis indicates varying degrees of excitation localization over benzenoid and quinoid substructures that are defined according to model A and B. The data listed in the Table II show consistently that the forbidden second $\pi-\pi^*$ transition ($S_0 \rightarrow S_2$) and the allowed fourth $\pi-\pi^*$ transition ($S_0 \rightarrow S_4$) have relatively low benzenoid character, while the quinoid character of these two transitions is large. Although this result is rather informative as compared to former phenomenological interpretations, the following deficiency of the analyses cannot be omitted: No con-

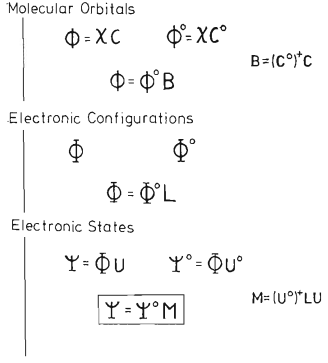

FIG. 1

Schematic Outline of the CA Procedure (Baba, Suzuki, Takemura 1969)

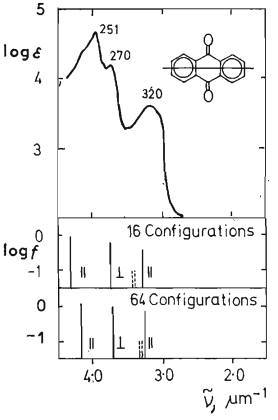

FIG. 2

Absorption Spectrum of 9,10-Anthraquinone in Heptane (absorption maxima in nm) and Electronic Transitions Calculated within Different Configuration Interaction Expansions

Full lines: allowed transitions; dashed lines: forbidden transitions; polarization of the transitions with respect to the lengthwise molecular axis.

clusion can be reached in this way about definite correlations between the individual anthraquinone absorption bands and those of the reference molecule. A sharp definition of the correlation pattern can only be achieved by the CA technique as outlined below.

TABLE I

Calculated and Experimental Spectral Data of 9,10-Anthraquinone

$\pi\pi^*$-States	Symmetry	16 Configurations[a]			64 Configurations[a]			Experimental data		
		λ, nm	lg f	P^b	λ, nm	lg f	P^b	λ, nm	lg ε	P^b
S_1	B_{3u}	301	—0·69	∥	306	—0·13	∥	320	3·72[c]	∥[d]
S_2	B_{1g}	295	forb.		301	forb.				
S_3	A_g	292	forb.		300	forb.				
S_4	B_{2u}	265	—0·24	⊥	269	0·04	⊥	270	4·32	⊥
S_5	B_{3u}	232	0·02	∥	240	0·13	∥	251	4·39	∥
S_6	B_{2g}	230	forb.		237	forb.				
S_7	B_{1g}	213	forb.		216	forb.				
S_8	B_{2u}	213	—0·62	∥	215	—0·29	∥			

[a] Transitions from the four highest-occupied to the four lowest-energy π-MOs. β_{CC} (within the benzene fragments): —2·318 eV, β_{CC} between benzene rings and the carbonyl groups: —1·9635 eV; [b] ∥ parallel to the long molecular exis, ⊥ perpendicular to the long molecular axis; [c] in heptane[18]; [d] Ref.[6].

TABLE II

Amount of Localization (in %) of 9,10-Anthraquinone According to the Ohta–Kuroda–Kunii (OKK) and Lusanov–Sukhorukov–Umanskii (LSU) Analysis

π—π^* Transitions	OKK Analysis, %			LSU Analysis, %		
	benzenoid	quinoid	anthracenoid	benzenoid	quinoid	antracenoid
$S_0 \rightarrow S_1$	37	14	75	80	43	89
$S_0 \rightarrow S_2$	25	38	73	70	71	85
$S_0 \rightarrow S_3$	26	19	69	79	34	87
$S_0 \rightarrow S_4$	19	47	54	62	71	75
$S_0 \rightarrow S_5$	34	15	82	81	45	92

OKK analysis relative to model C and D is not worth detailing here, but results relative to model E are contained in Table II. Fragmentation mode E can only be examined by OKK analysis, for both closed and open shell substructures result from the anthraquinone molecule in that case. The anthracenoid character is clearly highest for the fifth $\pi-\pi^*$ transition ($S_0 \rightarrow S_5$). Thus the formerly assumed correspondence between the most intense near UV absorption band of anthraquinone and that of anthracene gains some support from OKK analysis.

Configuration analysis of the state wave functions specifies the above mentioned relations: The r_M-values indicate a rather distinct appositeness of model A to D. (Table III). Due to the fact that strong π-bonds are broken according to model B and C, these models are less suited than model A and D. Model A suffers from the drawback that a relatively poor composite molecule description of the excited states is obtained. The best model of the four considered models presents model D. The r_M-values in Table III indicate a satisfactory reproduction of both the anthraquinone ground and excited states.

The distinct appositeness of the models has to be considered when a quantitative interpretation is attempted in limited configuration interaction expansions that are based on fragment orbitals LHM calculations. For qualitative interpretation purposes, however, each configuration analysis may be useful. Considered at the same time, the analysis provides a rather consistent picture about the electronic states which specifies the above discussed results of the electronic transition analysis. Only significant correlations are illustrated in Fig. 3.*

TABLE III

Appropriateness of Different Fragmentation Modes of 9,10-Anthraquinone according to the r_M-Values of the Configuration Analysis[a]

State	CA-Index r_M, %			
	model A	model B	model C	model D
S_0	90	47	72	89
S_1	70	26	44	80
S_2	70	25	40	78
S_3	72	33	41	79
S_4	74	24	43	80
S_5	72	24	42	76

[a] 16 Reference state wave functions.

* We refrain from presenting the full numerical results of these analyses. They are obtainable from one of the authors (J. F.).

The first $\pi-\pi^*$ transition (320 nm absorption band) arises from the L_b states of the benzene fragments (model A). The L_b states of the two fragments appear as excitonic combinations and the allowed first anthraquinone transition results from the in-phase combination of the L_b transitions. None of the higher excited electronic transitions of anthraquinone, however, are dominantly described by the excitonic combination of the L_a states of the benzene fragments. The calculated configuration mixtures contain considerable contributions of benzene-to-carbonyl charge transfer configurations. Hence, it is not surprising that model D enables a better correlative interpretation than model A, for reference is made to a joint benzene-carbonyl sub-

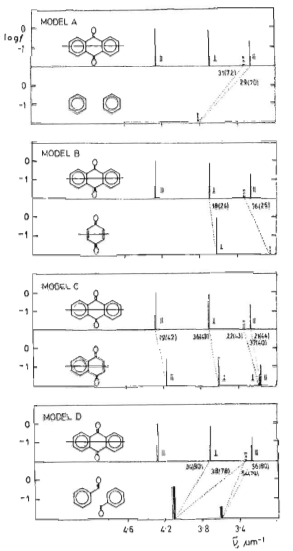

FIG. 3

Correlation between the Calculated Electronic Transitions of 9,10-Anthraquinone and those of Molecular Fragments According to PPP CA Calculations

The numbers indicate the contribution of the respective loccally excited electronic states to the anthraquinone excited states and, in parenthesis, the completeness of the projection (r_M in %). Sixteen reference state wave functions are considered. Any energy delocalization between localized reference state wave functions is not depicted in the figure.

structure. Whereas the first and third $\pi-\pi^*$ transitions are interpreted by the lowest energy benzoyl excited state (L_b-type excited state) according to this model, the forbidden second $\pi-\pi^*$ transition and the allowed fourth $\pi-\pi^*$ transition correlate with the second excited state of the benzoyl moiety (L_a-type excited state). However, the correlation of the higher excited states is less close than that of the lower excited states (lower r_M-value in Fig. 3). At any rate, configuration analysis reveals that the 320 nm band should be considered as L_b-type benzenoid band both with respect to model A and B. This conclusion supports the former phenomenological assignment which has been mentioned above. The ^1_sfifth excited anthraquinone state, however, is only described by a complex mixture of locally excited benzene states (L_b, B_b) or, alternatively, higher excited benzoyl states and CT states. The benzenoid character of the absorption band (250 nm) can therefore not be specified satisfactorily.

When looking for quinoid-type transitions, analysis according to model B should be consulted. The two lowest-energy *para*-benzoquinone excited states obviously dominate the excited states S_2 and S_4 of anthraquinone. Consequently, the forbidden $S_0 \rightarrow S_2$ and the allowed $S_0 \rightarrow S_4$ transition, which give rise to the 270 nm absorption band might be considered as quinoid transitions. This is accordant with the former assignment of the 270 nm band. However, because of the poor adequacy the projected wave function, this result should not be overestimated. Furthermore, the former classification was wrong in that the "quinoid band" of *I* at 270 nm correlates with the second $\pi-\pi^*$ absorption band of *para*-benzoquinone (240 nm), and not with the first $\pi-\pi^*$ absorption band (278 nm) as formerly assumed.

Close correlations have been found between the absorption bands of 9,10-anthraquinone and 1,4-naphthoquinone. As shown in Fig. 3, the 320 nm band is actually related for example, to the first $\pi-\pi^*$ absorption band of 1,4-naphthoquinone if only its parallel polarized component is considered. The configuration analysis suggests, moreover, definite correlations between the shorter wavelength absorptions, in particular between the 250 nm band of 9,10-anthraquinone and the 250 nm band of 1,4-naphthoquinone.

Whereas analysis only provides interpretations of excited states that are described by delocalized wave functions in terms of molecular subunits, direct calculation of the excited states from the functions of the molecular subunits way afford both a prediction of the term levels and an understanding of their genesis. However, the less appropriate the choice of the molecular fragments, the more likely the latter approach is to fail. In order to disclose this relationship, we repeated the calculation of anthraquinone starting from the respective fragments that are defined by the models A to D (LHM calculations). The dimension of the CI expansion was the same as used for the configuration analysis. The results of the PPP and LHM calculations are compared in Fig. 4. Again, the CA technique has been used to derive the correlation pattern between the term levels of the two separate calculations.

The results of this examination manifest the conclusion reached from analytical approach. The π-electronic states of anthraquinone are satisfactorily reproduced by LHM calculations that make use of the most appropriate model D. The LHM term level of lowest-energy excited states that account for intense $\pi - \pi^*$ absorptions are spaced similarly to the PPP term level.

They are constantly shifted, however, to higher energies. This shift in energy corresponds closely to the calculated so-called ground state depression energy. The horizontal arrow in Fig. 4 vizualizes the wavenumber shift which results from neglecting the depression energy. Neglect of this energy brings the absorption wavenumbers

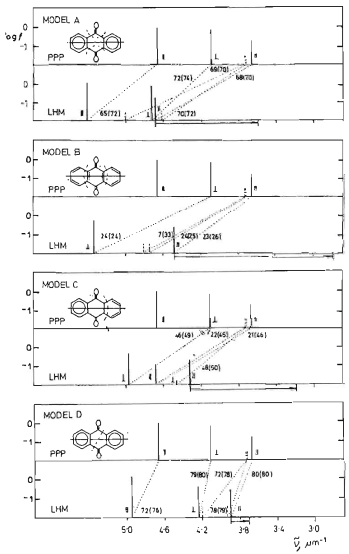

FIG. 4

Correlation between the Electronic Transitions of 9,10-Anthraquinone that Are Calculated by PPP and LHM Method according to CA Calculations

The numbers indicate the contribution of the corresponding reference electronic states and, in parenthesis, the projection (r_M in %). Sixteen reference state wave functions are considered. The horizontal arrow visualizes the shift of the lowest energy transition accompanied by neglect of the ground state depression energy.

calculated in the same region of the energy spectrum as found by the PPP method. The inappropriateness of model A and C is reflected in high ground state depression energies and in alterations of the term level sequence. Again, neglect of these energies considerably improves the position of the longest-wavelength absorptions. The results according to model D are surprising in that the term level sequence is still reproduced quite reasonably, although the model is highly unfavoured. The shortcoming of this calculation is, however, clearly evident when the predicted transition energies are considered. Even if the ground state depression energy was dropped, no accordance is to be reached in the wavenumber positions between the results of the LHM and PPP calculation.

The Anthraquinone Chromophore in Anthraquinone Derivatives

In order to disclose the nature of the anthraquinone chromophore, derivatives could also be considered by the above used model A to D. Then some of their absorption bands would have a certain benzenoid or quinoid character. A more attractive approach, however, consists in considering the π-system of the parent anthraquinone as a more adequate reference chromophore. Now the question can be raised, as to whether substituents only perturb the absorption bands of the parent chromophore or produce new absorption bands. This question is pursued in the following by the CA technique. The results of CA calculations of the mono-substituted anthraquinones *II* to *IV* are assembled in Table IV. According the r_M values the excited state wave functions of the substituted anthraquinones considered are satisfactorily reproduced by the 16-lowest-energy anthraquinone excited state wave functions and 4 CT configurations, in which the electron is either transferred from the anthraquinone fragment to the substituent (in *II*) or from the substituent to the anthraquinone fragment (in *III* and *IV*). Only the contributions of the locally excited states S_1 to S_5 of the anthraquinone parent chromophore (labelled by S_1^0 to S_5^0) are assembled in Table IV. Obviously, definite term levels of substituted anthraquinones are closely related to those of the parent chromophore, whereas some higher energy levels, which are expected to give the near UV absorption bands, cannot be understood by the five lowest energy level of *I* only. Moreover, there are energy levels in which the sum of the CT configurations is larger than the contribution of any singly excited state. These are higher excited states in the case of 2-nitroanthraquinone, *e.g.* the fifth excited state (S_5), but the lowest energy states in the case of 1-amino- and 2-aminoanthraquinone (S_1). This outcome might be considered as a support of the former charge transfer classification of the colour bands of *III* and *IV*. However, it should not be overlooked that locally excited states non-negligibly contribute to the lowest excited states of both compounds. This is predominantly the state S_1 of *I* (S_1^0) for 1-aminoanthraquinone, but the state S_2 of *I* (S_2^0) for 2-aminoanthraquinone. The different intensity of *III* and *IV* reflects the distinct nature of the contributing locally

TABLE IV

Calculated and Experimental Absorption Wavelengths of Substituted Anthraquinones and Results of the PPP–CA Calculations[a]

λ, nm (log *f*)		S_1^0	S_2^0	S_3^0	S_4^0	S_5^0	CT	r_M		λ, nm (log ε)
					Compound *II*					
306 (—0·63)	S_1	83	1	1	—	1	3	89		323 (3·72)[b]
301 (—1·33)	S_2	1	48	37	—	—	3	90		
298 (—1·64)	S_3	1	31	36	—	—	15	85		
273 (—0·17)	S_4	—	—	—	68	—	14	89		
247 (—0·16)	S_5	—	3	—	14	5	29	86		258 (4·62)
235 (—0·58)	S_6	1	—	2	—	44	16	88		
232 (—0·67)	S_7	—	1	3	3	23	22	85		
224 (—1·24)	S_8	1	—	—	—	—	29	90		
					Compound *III*					
397 (—0·65)	S_1	28	1	17	—	1	32	83	453 (3·17)[c]	476 (3·72)[d]
299 (—1·88)	S_2	—	22	38	18	1	2	81	304 (2·80)	307 (3·64)
297 (—1·77)	S_3	—	12	37	29	—	2	82		
274 (—0·87)	S_4	—	5	—	55	—	9	82	276 (3·28)	270 (3·98)
257 (—0·24)	S_5	—	—	—	21	1	19	83		244 (4·44)
250 (—1·04)	S_6	2	—	1	—	14	27	84		
231 (—0·16)	S_7	—	—	—	—	52	—	81		
225 (—0·52)	S_8	—	—	—	1	1	32	83		
					Compound *IV*					
358 (—0·71)	S_1	14	23	8	6	—	31	85	412 (3·58)[c]	449 (3·55)[d]
304 (—2·18)	S_2	32	27	11	2	1	10	85	328—340 (3·87)	
298 (—0·92)	S_3	29	—	53	—	—	1	84		
274 (—0·35)	S_4	—	18	—	57	3	4	84	318 (4·24)	298 (4·22)
258 (—0·12)	S_5	3	—	6	10	27	16	84	286 (4·36)	
233 (—0·74)	S_6	—	—	—	—	1	22	84		
230 (—0·45)	S_7	—	—	—	—	35	4	84	239 (4·4)	244 (4·44)
220 (—1·83)	S_8	—	—	—	—	1	31	84		

[a] S_1^0, S_2^0, ... and CT denote the amount of locally excited anthraquinone states and lowest-energy amino-to-anthraquinone CT-states, respectively, in %. The r_M-values indicate the completeness of the projection. The wave functions of the composite molecule reference states are generated from 16 singly excited states of *I* and 4 (8) CT-configurations arising from excitation from one (or two) lone pair orbital of nitrogen to four lowest-energy unoccupied MO's of *I*. [b] In methanol[13], [c] in dioxane/heptane[18], [d] in ethanol[18].

excited states which give rise either to an allowed transitions in the parent compound (S_1^0) or a forbidden one (S_2^0).

Table IV also shows, that the absorption wavelengths of amino-substituted anthraquinones are not well reproduced by PPP calculations which make use of a standard parametrization. The method generally predicts the colour bands at too short wavelengths. Since the numerical data can be improved by increasing the donor capacity of the nitrogen and the acceptor capacity of the oxygen, an underestimation of the substituent-to-anthraquinone charge transfer is suggested. Although the main conclusions might hardly be affected if the calculations were repeated with a more proper parametrization, we restrain here from a more detailed discussion of theoretical data. Based on polarization spectra of aminoanthraquinones, this problem will be considered in a forthcoming paper.

Indanthrone (*V*) presents more complex anthraquinone derivative. The structure was the subject of much controversy, but the molecular structure advanced in the pioneering work of Scholl[40] has been confirmed spectroscopically[41]. The blue indanthrone displays a colour band centered at about 680 nm (ref.[42]).

A strong colour band has been calculated at long wavelengths but the calculated absorption wavelength is considerably too small (*cf.* Table V). Due to the fact that nitrogen atoms are strongly involved in the electronic delocalization, the composite molecule description of the electronic ground state (S_0), based on anthraquinone substructures, is poor (model G). Similarly, Dähne's model H fails completely because the four subunits defined this way merge relatively strong into each other. Model I which involes 2-aminoanthraquinone subchromophore, is somewhat more favoured over the above discussed fragmentation mode.

TABLE V

Results of PPP–CA Calculations of Indanthrone (*V*) and Isoindanthrone (*VI*)

Compound	Exp. values λ, nm (colour)	Calc. values λ, nm (log *f*)		r_M Values, %		
				model G[a]	model H[a]	model I[b]
V			S_0	73	27	77
	740, 690, 643[c]	536 (—0·12)	S_1	49	13	63
	(blue)	323 (—1·29)	S_5	20	10	33
VI			S_0	76		79
	(green)	541 forb.	S_1	36		58
		440 (—0·82)	S_2	35		63

[a] 36 Reference state wave functions; [b] 16 reference state wave functions; [c] in chloroform[42].

This fragmentation mode also has the advantage that the isomeric isoindanthrone (*VI*) can be constructed from the same substructure. The green pigment *VI* has been prepared[43].

The theoretical results of *VI* differ in two aspects from those of *V*. First, whereas *V* is calculated to absorb intensively at long wavelengths, the lowest-energy transition of *VI* is symmetry-forbidden. Secondly, the first allowed transition of *VI* is not expected until 400 nm. This absorption should impart a strong yellow component to the observed colour. This may account for the difference in visual colour observed between indanthrone (blue) and isoindanthrone (green).

The different transition probability of the lowest energy transition follows from the combination of the frontier orbitals of 2-aminoanthraquinone. Whereas the resulting HOMO and LUMO of *V* differ in their symmetry behaviour with respect to the inversion centre, giving rise to a $g-u$ type transition, a $g-g$ type transition results for *VI*. The latter transition is forbidden according to the "parity forbiddeness".

CONCLUSIONS

Configuration analysis presents a suited theoretical method which enables the discussion of the anthraquinone absorption bands in terms of their constituent parts. The longest wavelength absorption band at 320 nm is actually localized at the benzene fragments (benzenoid band). The electronic excitation is mainly due to L_b excited stated of benzene. The second benzenoid band at 251 nm has a more complex origin. In that case, the benzene-to-carbonyl charge transfer plays more important role. Although the interpretation of 270 nm band as quinoid band also furnished some evidence, the correlation proved to be rather poor.

Analysis supports the advantage of describing anthraquinone in terms of two benzoyl halves. In good harmony, the term level sequence and energy position of the $\pi-\pi^*$ excited states of anthraquinone are satisfactorily reproduced by the equivalent synthetic approach (LHM calculations).

The spectra of substituted anthraquinones can be well interpreted in terms of local anthraquinone excitations and CT excitations. CA calculations have confirmed the CT character of the lowest-energy excitation, but have indicated, at the same time, certain admixtures of the lowest-energy anthraquinone excited states. The detailed assignment and interpretation of the aminoanthraquinone absorption bands is, however, hampered by the poor numerical agreement between theoretical and experimental absorption wavelengths. A more detailed study about aminoanthraquinones is now in progress.

REFERENCES

1. Fain V. Ya.: *Tables of Electronic Spectra of Anthraquinone and its Derivatives.* Khimiya Leningrad 1970.
2. Thomson R. H.: *Naturally Occurring Quinones.* Academic Press, New York 1971.
3. Moran J. J., Stonehill H. J.: J. Chem. Soc. *1957*, 765.
4. Titz M., Nepraš M.: This Journal *37*, 2674 (1972).
5. Kuboyama A., Matsuzaki S., Takagi H., Arano H.: Bull. Chem. Soc. Jap. *47*, 1604 (1974).
6. Novák A., Titz M., Nepraš M.: This Journal *39*, 1532 (1974).
7. Giovanelli K. H., Dehler J., Hohlneicher G.: Ber. Bunsenges. Phys. Chem. *75*, 864 (1971).
8. Edwards T. G.: Theor. Chim. Acta *30*, 267 (1973).
9. Olbrich G., Polansky O. E., Zander M.: Ber. Bunsenges. Phys. Chem. *81*, 692 (1977).
10. Drott H. R., Dearman H. H.: J. Chem. Phys. *47*, 1896 (1967).
11. Scott J. D., Watson W. H.: J. Chem. Phys. *49*, 4246 (1968).
12. Platanova N. V., Popov K. R., Smirnov L. V.: Opt. Spektrosk. *26*, 357 (1969).
13. Peters R. H., Summer H. H.: J. Chem. Soc. *1953*, 2101.
14. Labhart H.: Helv. Chim. Acta *40*, 1410 (1957).
15. Yoshida Z., Takabayashi F.: Tetrahedron *24*, 933 (1968).
16. Hartmann H., Lorentz E.: Z. Naturforsch. *7a*, 360 (1952).
17. Egerton G. S., Roach A. G.: J. Soc. Dyers Colour. *74*, 401 (1958).
18. Shcheglova N. A., Shigorin D. N., Dokunikhin N. S.: Zh. Fiz. Khim. *42*, 2724 (1968).
19. Inoue H., Hoshi T., Yoshino J., Tanizaki Y.: Bull. Chem. Soc. Jap. *45*, 1018 (1972).
20. Inoue H., Hoshi T., Yoshino J., Tanizaki Y.: Bull. Chem. Soc. Jap. *46*, 380 (1973).
21. Zaitsev B. E., Allenov V. M.: Zh. Prikl. Spektrosk. *20*, 109 (1974).
22. Pilipenko A. T., Savranskii L. I.: Opt. Spektrosk. *28*, 808 (1970).
23. Morton R. A., Earlam W. T.: J. Chem. Soc. *1941*, 159.
24. Singh I., Ogata R. T., Moore R. E., Chang C. W. J., Scheuer P. J.: Tetrahedron *24*, 6053 (1968).
25. Popov K. R., Platonova N. V., Smirnov L. V.: Opt. Spektrosk. *27*, 1097 (1972).
26. Dähne S., Leupold D.: Angew. Chem. *78*, 1029 (1966).
27. Spruit C. J. P.: Rec. Trav. Chim. *68*, 325 (1949).
28. Zander M.: Ber. Bunsenges. Phys. Chem. *71*, 424 (1967).
29. Hill R. R., Mitchell G. H.: J. Chem. Soc. B *1969*, 61.
30. El Ezaby M. S., Salem T. M., Zewait A., Issa R.: J. Chem. Soc. *1970* B, 1293.
31. Fabian J.: Z. Phys. Chem. (Leipzig) *258*, 81 (1977).
32. Fabian J., Mehlhorn A., Fratev F.: Unpublished results.
33. Fabian J.: J. Signalaufzeichnungsmaterialien *6*, 307 (1978).
34. Baba H., Suzuki S., Takemura T.: J. Chem. Phys. *50*, 2078 (1969).
35. Fabian J., Zahradník R.: Wiss. Z. Techn. Univ. Dresden *26*, 315 (1977).
36. Ohta T., Kuroda H., Kunii T. L.: Theor. Chim. Acta *19*, 167 (1970).
37. Lusanov A. V., Sukhorukov A. A., Umanskii V. E.: Teor. Eksp. Khim. *10*, 456 (1974).
38. Longuet-Higgins H. C., Murrell J. N.: Proc. Phys. Soc. A *68*; 601 (1955).
39. Giovanelli K. H., Hohlneicher G., Straub P. A.: Ber. Bunsenges. Phys. Chem. *75*, 857 (1971).
40. Scholl R.: Ber. Deut. Chem. Ges. *36*, 3410 (1903).
41. Weinstein J., Meritt Ch.: J. Amer. Chem. Soc. *81*, 3759 (1959).
42. Schorer M., Dörr F.: Ber. Bunsenges. Phys. Chem. *68*, 478 (1964).
43. Leete E., Ekechukwu O., Delvigs P.: J. Org. Chem. *31*, 3734 (1966).
44. Nepraš M., Titz M.: Int. J. Quantum Chem. *16*, 543 (1979).